Strader, J., et al., 2012, *Nature*, **490**, 71
Szomoru, A., 2008, *PoS["IX EVN SYmposium"]40*
Tendulkar, S.P. et al., 2017, *ApJ*, **834**, L7
Tetarenko, B.E. et al., 2016, *ApJ*, **825**, 10
Thornton, D. et al., 2013, *Science*, **341**, 53
Tingay, S.J. et al., 1995, *Nature*, **374**, 141
Tudose, V. et al., 2007, *MNRAS*, **375**, L11
van Velzen, S. et al. 2016, *Science*, **351**, 62
Varenius, E. et al. 2019, *A&A*, **623**, A173
Wellons, S. et al. 2012, *ApJ*, **752**, 17
Willems, B. et al., 2005, *ApJ*, **625**, 324
Woosley, S. & Bloom, J. 2006, *ARA&A*, **44**, 507
Wysocki, D. et al., 2018, *PhRvD*, **97**, 043014
Yang, J. et al., 2016, *MNRAS*, **462**, 66
Yungelson, L. et al., 2006, *A&A*, **454**, 559
Zauderer, B.A. et al., 2011, *Nature*, **476**, 425
Zhang, & W., MacFadyen, A., 2009, *ApJ*, **698**, 1261
Zhou, B. et al., 2014, *Phys. Rev. D.*, **89(10)**, 107303
Zrake, J., Xie, X., & MacFadyen, A., 2018, *ApJL*, **865**, L2

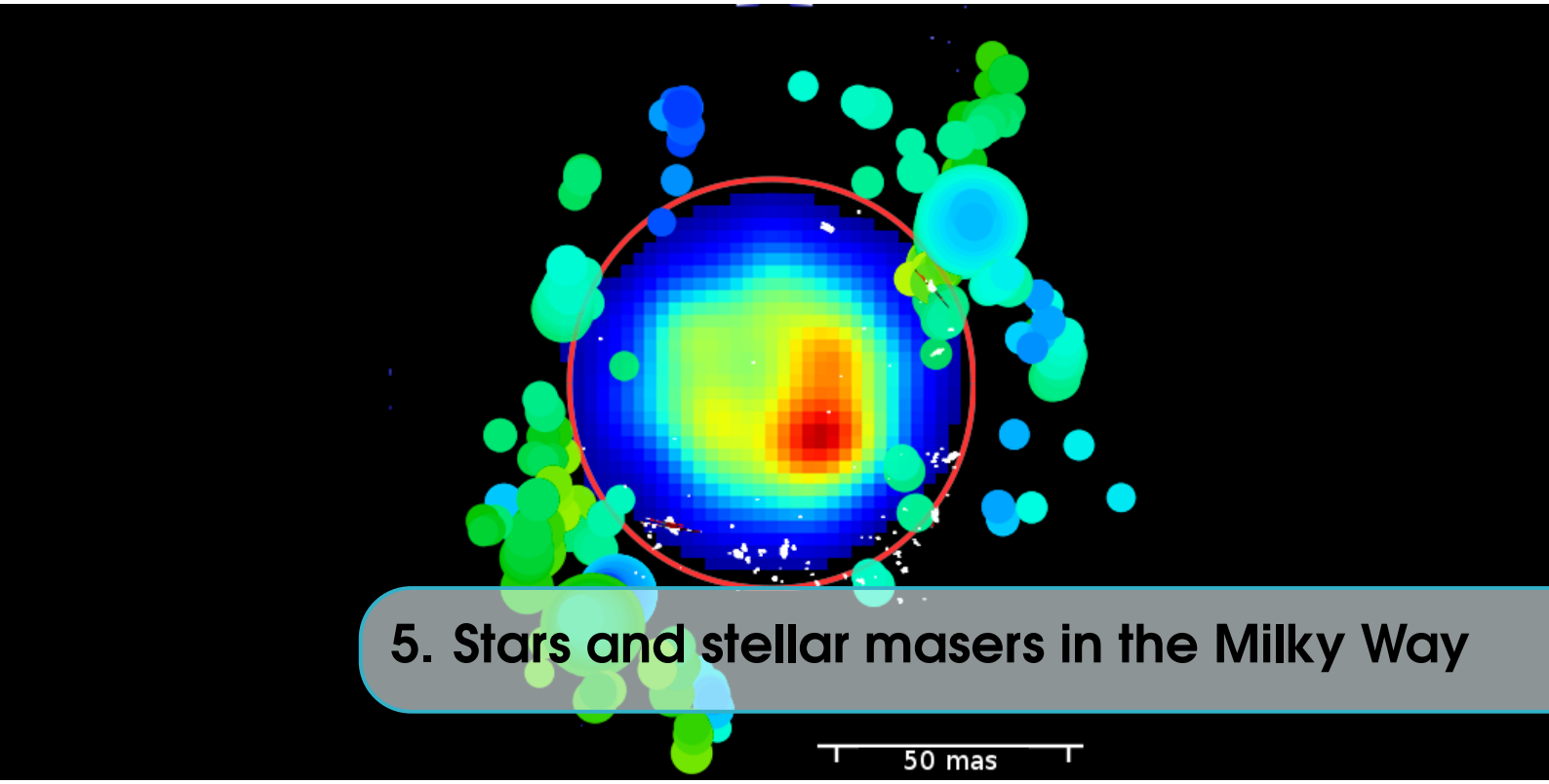

5. Stars and stellar masers in the Milky Way

Over the last decades, our understanding of the stellar astrophysics has been greatly enhanced by observations of radio interferometers. Although stars are not profuse radio emitters, the increasing resolution and higher sensitivity of new instruments have provided valuable insights on every stage of the stellar evolution. Accordingly, the contribution of VLBI in this field materialises in a variety of discoveries including stellar flares, structures of the magnetic coronae, colliding-wind binaries, low-mass objects near the substellar transition, as well as the measurements of positions, proper motions, parallaxes, and orbital motions with accuracies of a fraction of a milliarcsecond. The first part of this chapter is therefore devoted to the wealth of astrophysical phenomena, and other spin-offs, related to stellar continuum studies. The second section of this chapter will describe spectral line observations of various masing molecules that constitute the VLBI Galactic maser science. Masers appear mostly in star-forming regions and in envelopes of evolved stars. High sensitivity studies of maser emission at milliarcsecond resolution, particularly from OH, H_2O, CH_3OH and SiO molecules, in the radio and millimetre domain provide one of the best existing tools for uncovering the kinematics and the physical conditions of regions that are hidden in dense, high extinction, environments. Maser structures, being compact and non-thermal, are also ideal astrometry targets with which one can study the furthest regions in the Galaxy and Galactic structure itself. Finally, the technical requirements and synergies for star and stellar maser observations are presented.

Chapter image credit: Diverse radio emission of W Hya, the Mira-type variable star in the constellation Hydra. The 338 GHz continuum emission detected by ALMA (Vlemmings et al. 2017), the 22 GHz continuum marked by the red circle (Reid & Menten 1990. 43 GHz SiO masers marked by white contours with polarisation "E" vectors (Cotton et al. 2008) and 22 GHz water masers marked by colourful spots (Richards et al. 2012) – reproduced with permission ©ESO.

5.1 Stellar evolution and planetary systems

5.1.1 Pre-main sequence stars

Protostellar radio jets

Accretion disks and collimated outflows (jets) are intrinsically associated with the star-formation process. In particular, the youngest, deeply embedded protostars are usually radio sources of free-free emission that trace the (partially) ionised region, very close to the exciting star (10-100 AU), where the outflow phenomenon originates, and are referred to as "thermal radio jets" (see Anglada et al. 2015, 2018 for recent reviews). In more evolved low-mass stars the radio emission is dominated by a non-thermal (gyrosynchrotron) process (Feigelson & Montmerle 1985) produced in their active magnetospheres; these compact non-thermal sources are excellent tools for the determination of accurate parallaxes using VLBI observations (e.g., Kounkel et al. 2017; see below).

Thermal radio jets are present in young stars across the stellar spectrum, from O-type protostars (Garay et al. 2003) and possibly to proto-brown dwarfs (Palau et al. 2014). This radio emission is relatively weak, and correlated with the bolometric luminosity. The observed centimetre radio luminosities (taken to be $S_\nu d^2$, with d being the distance) go from $\sim$100 mJy kpc^2 for massive young stars to $\sim 3 \times 10^{-3}$ mJy kpc^2 for young brown dwarfs (Anglada et al. 2018). Nevertheless, given the large obscuration present towards the very young stars, the detection of the radio jet provides so far the best way to obtain their accurate positions. Dynamical timescales of these radio jets are short, and these observations provide information on the physical properties, direction and collimation of the gas ejected by the young system in the last few years.

VLBI observations could in principle trace details of the jets at very small scales. An angular resolution of 1 mas in a nearby radio jet (d= 200 pc) would resolve details of the jet structure with a physical size of 0.2 AU, which is of the order of the size of the launch region. However, the thermal nature of the emission hinders the study with the highest angular resolution. A maximum intensity of only $\sim$7 μJy/beam (assuming optically thick emission at 10,000 K) is expected for a beam of 1 mas, which would require very sensitive observations.

Interestingly, non-thermal synchrotron emission is also present in several protostellar jets. This non-thermal emission is usually found in relatively strong radio knots, away from the jet core, showing negative spectral indices at centimetre wavelengths (Rodríguez-Kamenetzky et al. 2017). The synchrotron nature of the emission was confirmed with the detection and mapping of linearly polarised emission in the HH 80-81 jet (Carrasco-González et al. 2010), establishing a link with the AGN and microquasar relativistic jets. Although velocities of protostellar jets are non relativistic, several theoretical studies show that the observed synchrotron emission can be produced by a small population of relativistic particles that have been accelerated in the strong shocks in protostellar jets (e.g., Araudo et al. 2007). Possible compact knots in these non-thermal knots are potential targets for future VLBI studies.

Protoplanetary / debris disks

The radio regime is unique for studying proto-planetary discs, the material out of which protostars and their planets are formed. Data from the Atacama Large Millimeter/submillimeter Array (ALMA) has proven that discs are not smooth flat plates of dust and gas, but highly complex in structure, and stirred by planet formation. The inner few AU of these disks, however, are opaque at millimetre wavelengths, and despite ALMA's high angular resolution, mm/submm interferometers cannot detect emission from the mid-plane of the disk, where planets are expected to form. In contrast, radio continuum arises from optically thin blackbody radiation, directly tracing the solid mass held

in large grains. Grains are poor emitters at wavelengths above their circumference, so only radio emission can tell if 'pebbles' are present, crucial to further aggregation into planets. The current state-of-the-art is to map the inner disc, and spatially separate the radio emission of the jets of young stars (a complexity that has plagued low-resolution studies). This arena with JVLA and especially *e*-MERLIN will progress into SKA (and precursors) studies. The next phase is to study the very fine details of material flowing into planetary cores, hinted at by ALMA, and ideally matched to milliarcsecond EVN scales. The science goals are to understand how planets build up mass and migrate within the disc, via resolving the Hill accretion sphere, spiral arms around the planet within disc gaps, etc. As the dust signal is very faint because of the frequency-squared or steeper spectrum, such observations are very challenging for present-day EVN. For example, the HL Tau b proto-planet candidate (Greaves et al. 2008) is expected to have $\sim 5\mu$Jy total flux at C-band. Zhu et al. (2018a, b) discuss the detectability of disks and jets associated with proto-planets. Their results show that sensitivities well below 1 μJy are required to attempt this kind of studies at centimetre wavelengths. The combination of *e*-MERLIN with the shortest EVN baselines may help to resolve the detailed processes. Increases to collecting area and bandwidth are therefore highly important.

In a few massive young stellar objects there is evidence that the associated centimetre source actually traces a photoionised disk (e.g., Hoare 2006, Reid et al. 2007). These objects show a similar centimetre spectral index to that of jets and are identified in terms of other criteria, such as their orientation with respect to the outflow axis or their radio luminosity relative to the bolometric luminosity. Ionised disks can also be present in the case of young low mass stars. The high resolution images of GM Aur presented by Macías et al. (2016) show that, after subtracting the expected dust emission from the disk, the centimetre emission from this source is composed of an ionised radio jet and a photoevaporative wind arising from the disk perpendicular to the jet. It is believed that extreme-UV (EUV) radiation from the star is the main ionising mechanism of the disk surface.

Clusters and star forming regions

Although star-formation has been observed and studied throughout the Milky Way and in many external galaxies, our current understanding of star-formation is largely based on the careful study of less than a dozen benchmark regions located within a few hundred parsecs of the Sun –Taurus and Orion are, perhaps, the best known of these regions. Indeed numerous detailed surveys have been performed at X-ray, infrared, microwave and radio wavelengths to characterise the stellar populations and the ISM content of these regions (e.g. Bally 2008, Muench et al. 2008, O'Dell et al. 2008 and Kenyon et al 2008 for reviews of such surveys of Orion and Taurus). As a result of the recent detailed imaging of protoplanetary disks in the same regions by ALMA (e.g. HL Tau in Taurus or Elias 2-27 in Ophiuchus; ALMA partnership et al. 2015, Perez et al. 2016), they are also quickly becoming the benchmark regions for the study of planet formation.

VLBI astrometric observations can readily provide position measurements accurate to better than 0.1 mas even for modest signal-to-noise detections (Reid & Honma 2014). As a consequence, multi-epoch VLBI observations appropriately scheduled over a time period of a few years can provide trigonometric parallax measurements accurate to 10 μas or better, and proper motions accurate to a few tens of μas yr^{-1}. This is comparable with the expected performance of the *Gaia* satellite. For objects within a few hundred parsecs, this yields distances and tangential velocities accurate to better than a few percent. In addition, VLBI observations at radio wavelengths are immune to dust along the line of sight, so accurate distance and velocity measurements can be obtained even for objects that are deeply enshrouded in dust, such as young stars in star-forming regions.

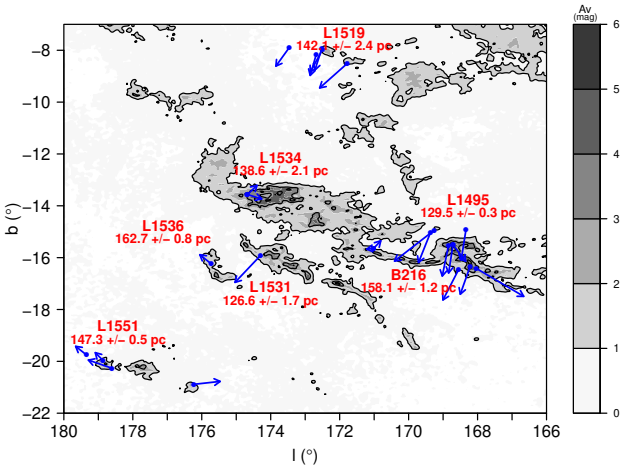

Figure 5.1: Three-dimensional structure of the Taurus star-forming regions (adapted from Galli et al. 2018). The underlying grey-scale image shows the extinction map derived by Dobashi et al. (2005) in Galactic coordinates. The different dust clouds in the region are indicated, together with their distance measured though VLBI astrometric observations. The blue arrows correspond to the proper motions (also determined from VLBI observations) measured in the Local Standard of Rest (LSR). Adapted from Galli et al. (2018). ©AAS. Reproduced with permission.

Taking advantage of this situation, the Gould's Belt Distances Survey (GOBELINS; Loinard 2013) was carried out to measure the distance and proper motion of a representative sample of young stars in five of the most prominent star-forming regions within 500 pc of the Sun (Taurus, Perseus, Ophiuchus, Orion and Serpens). From these observations, the mean distance, the three-dimensional structure, and the internal kinematics of each region could be obtained (Ortiz-León et al. 2017a, 2017b, 2018; Galli et al. 2018; Kounkel et al. 2017). Additional regions, such as Monoceros or LkHα101, were considered in complementary observations (e.g. Dzib et al. 2016, 2018). Together, these observations have resulted in great improvements in our knowledge of the distribution of nearby star formation (see Fig. 5.1 for the example of the three-dimensional structure of the Taurus region), and have sometimes revealed large errors in previous estimates. For instance, the Serpens core was usually accepted to be at a distance of 260 pc (Straižys et al. 1996, 2003) but the GOBELINS survey revealed that it is located nearly 70% farther at 436 ± 9 pc (Ortiz-León et al. 2017b). This implies, in particular, that previously estimated luminosities for objects in that region are underestimated nearly by a factor of 3.

One of the interesting by-products of the GOBELINS survey has been the resolution of nearly two dozen very tight young binary stellar systems (with separations between a few and a few tens of mas – Ortiz-León et al. 2017a, 2017b; Galli et al. 2018; Kounkel et al. 2017).[1] In such cases, the displacement of the stars on the celestial sphere can be modelled as a combination of their trigonometric parallax and their systemic and orbital motions. The characterisation of the orbital motion enables the determination of masses through Kepler's law. Using orbital motions to estimate masses of stars in binary systems has, of course, been used for many decades. For young stars, near-infrared observations have typically been preferred (e.g. Ghez et al. 1993), and increasingly

[1] See also Torres et al. (2012) for an earlier case.

sophisticated techniques (speckle interferometry, adaptive optics or aperture masking) have been developed to resolve ever tighter systems (currently down to about 10 mas). VLBI observations at centimetre wavelengths have a typical resolution of about 1 mas, so they can resolve systems that near-IR observations cannot. VLBI observations have two additional fundamental advantages over near-IR imaging. The first one is that they enable a simultaneous determination of the orbital motion **and** the trigonometric parallax. As a consequence, the binary systems resolved by VLBI observations automatically also have very accurately known distances. Near-IR imaging, on the other hand, measures the angular semi-major axis of the orbits, but needs to rely on independently measured (and often quite uncertain) distances to transform this angular measurement to a physical distance. Since the mass depends on the cube of the semi-major axis, even a small error on distance can result in a very significant mass error. The second important advantage of VLBI over near-IR imaging is that it delivers masses for the individual stars in the system and not only the total system mass. This is because VLBI data provide positions of the individual stars measured relative to a background calibrator (normally a quasar). This implies that the relative motion between the individual stars and the centre of mass of the system can be measured, and therefore also the mass ratio. The mass measurements of young stars provided by VLBI observations are fundamental to constrain pre-main sequence evolutionary models (see below).

The GOBELINS results described above are based on only about 100 individual VLBI parallax and proper motion measurements. An increase in sensitivity of VLBI arrays would enable a major step forward. At the current level of sensitivity, VLBI observations can only detect 10 to 20% of the young stars known to exist in star-forming regions at a few hundred parsecs. Given the known luminosity function of these sources (Ortiz-León et al. 2017a), an increase in sensitivity by a factor of 10 would roughly multiply by three the number of detectable sources, and bring the detection fraction to about 50%. This would have fundamental implications for the determination of the three-dimensional structure and internal kinematics of nearby star-forming regions, and would enable similar measurements to be carried out for regions that are significantly farther.

Calibration of PMS evolutionary models

Stellar evolution models allow us to understand the different phases that the stars cross throughout their existence. As a general rule, the predictions provided by these models fit the observations well and, therefore, can be considered a reliable source of scientific information. This is particularly useful to estimate fundamental parameters of the stars, such as the mass and radius, from theoretical luminosity-based relationships (e.g., Baraffe et al. 1998; Chabrier et al. 2000). The calibration of these stellar evolution models is important, but it is crucial in the case of young, low-mass objects, since these models are frequently used to determine the masses of planets and brown dwarfs. The study of binary stars belonging to young, moving groups (whose main feature is the common age of their members; Zuckerman & Song 2004; Torres et al. 2008) is a reasonable approach to increase the number of PMS stars with dynamically determined masses, as these have shown to be suitable benchmarks to calibrate models. In recent years, several of these moving groups have been discovered (Pictoris, Tucana-Horologium, TW Hydrae, Columba, Carina, Argus, and AB Doradus moving groups); both LBA and EVN astrometric observations have determined or refined the distance and orbital motion of some multiple systems belonging to the previous groups (AB Dor A/C, AB Dor Ba/Bb, or HD 160934 A/c; Guirado et al. 1997; Azulay et al. 2015; 2017), helping to alleviate the deficient observational status of dynamical masses of PMS stars, and therefore imposing strong constraints to stellar evolutionary models (see Fig. 5.2).

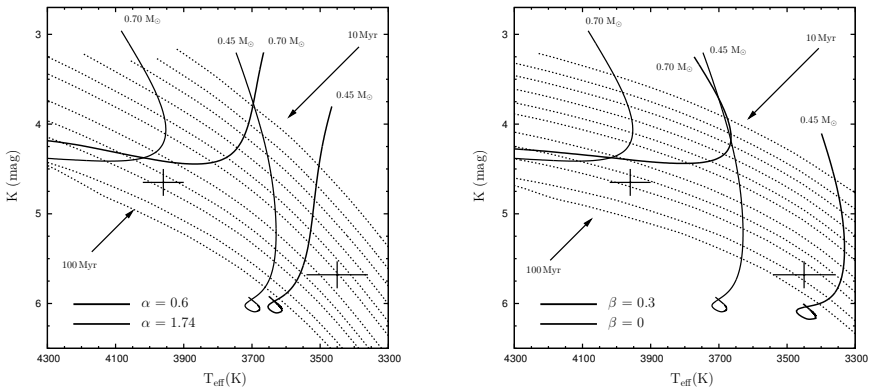

Figure 5.2: Example of comparison of the dynamical masses of the HD 160934 A/c system with the predictions of the models of Tognelli et al. (2011). Both isomasses (solid lines) and isochrones (dashed lines) are plotted. The highlighted tracks are those nearest to the dynamical mass values (0.70 ± 0.07 and $0.45\pm0.04\,M_\odot$ for components A and c, respectively). (left) Effect of an internal magnetic field, simulated by using a value of the mixing length $\alpha = 0.6$. The isomasses of a standard solar value $\alpha = 1.74$ are also plotted for comparison. (right) Effect of stellar spots, computed for an effective spot coverage of $\beta = 0.3$ (Somers & Pinsonneault 2015). The isomasses for $\beta = 0$ (standard models with no spots) are also plotted for comparison. These and other model comparisons can be seen in Azulay et al. (2017). Reproduced with permission ©ESO.

Although the previous projects are limited to a handful of stars, it constitutes a foundation for future studies of the stellar and substellar evolution using the new, more sensitive radio interferometers. At present, the EVN is an excellent tool for these studies, although higher resolution, better sensitivity, and larger monitoring speed will allow the access to a much larger number of members belonging to the moving groups discovered. Extension of the EVN to the southern hemisphere, through the development of the African VLBI Network (AVN) is particularly welcome, as the majority of the moving groups are located in the southern sky.

5.1.2 Main sequence stars

Stellar rotation coupled with convective motions generate strong magnetic fields responsible for a multitude of phenomena including coronal loops, radio flares, or stellar spots.

Flares / coronal mass ejections

There is substantial bibliography showing that many late type (F, G, K, M) stars display incoherent radio flares (e.g. Güdel et al. 1998), which evidences the presence of midly relativistic electrons in magnetic fields. On the other hand, flares produced by a coherent radiation mechanism, abundant on magnetically active M dwarfs, carry profound information on the conditions of the corona during magnetic reconnections or coronal mass ejections (CMEs). The studies of coherent radio bursts have been bandwidth limited, at least until recent upgrades of instruments as the JVLA, which have allowed detailed stellar dynamic spectroscopy (studies of the spectral evolution over time) spanned over a wide spectral range (Güdel et al. 1989; Bastian et al. 1998). These studies have provided evidence of both plasma density and magnetic field gradients which translate to coronal plasma motion on active M dwarfs (Osten & Bastian 2006, 2008). Hence, the radio emission can be

monitored across multiple coronal scale heights, which helps to identify the mechanism producing these bursts. The role of a sensitive VLBI array would be to image the non-thermal corona, seeking for resolved gyrosynchrotron emission, and tracing the possible motions of coronal plasma. In fact, JVLA and VLBA combined observations have already been carried out on popular flare stars such as AD Leo, UV Ceti and YZ CMi (Villadsen et al. 2017), enabling the simultaneous measurement of the dynamic spectra and the spatial offset between flaring and quiescent emission. This high-resolution search for spatial signatures of CMEs is therefore a perfect complement to the dynamic studies of the stellar corona. Villadsen et al. (2017) also emphasise the relevance of CME's for future astrobiology projects, as they are predicted to cause significant mass loss from planetary atmospheres (Khodachenko et al. 2007, Lammer et al. 2007) of possible companions to M dwarfs. The emission of energetic particles may produce drastic changes in molecular chemistry of planetary atmospheres, affecting in particular biomarkers like ozone (Segura et al. 2010).

Ultracool Dwarfs

Radio observations play an important role in understanding the processes involved in the formation and evolution of stellar and substellar objects. In particular, radio emission studies of ultracool objects (late M, L, and T objects; e.g. Matthews 2013) are relevant to probe the magnetic activity of these objects and its influence on the formation of disks or planets. Moreover, the study of ultracool dwarfs may open a suitable route to the detection of radio emission of exoplanets: meanwhile no exoplanet has yet been detected at radio wavelengths, an increasing number of ultracool objects (Hallinan et al. 2008; Pineda et al. 2017; Guirado et al. 2018) show substantial evidence of radio emission at GHz frequencies in objects with spectral types as cool as T6.5 (Kao et al. 2016; 2018). This radio emission is consistent with incoherent gyrosynchrotron with at least another pulsed, auroral emission, produced by electron cyclotron maser (ECM) instabilities, whose periodicity matches the stellar rotation rate. This evidences the persistence of magnetic activity ($\sim$kG) in very low mass objects. Moreover, radio observations become a unique tool to probe the magnetic properties of these objects, as other indicators such as Hα or X-rays decline for such late spectral types.

However, although rapid rotation seems to be an essential ingredient to generate kG magnetic fields, the precise mechanism still remains unresolved. The fully convective nature of ultracool dwarfs (UCDs) does not allow the solar-type $\alpha\Omega$ dynamo, operating at the shearing interface between the radiative and convective zones (Parker 1955), to generate and amplify the observed magnetic fields. Since UCDs simulations have not been investigated so far, much emphasis is needed on finding observational constraints for the magnetic field properties. Zeeman spectroscopy requires very high signal-to-noise ratios and low/moderate rotation velocities (Reiners & Basri 2007). These conditions are hardly ever met in UCDs, therefore, observational constraints on the scale, geometry, and origin of the magnetic fields, such as those provided by VLBI, are essential. In this context, VLBI observations of ultracool dwarfs have contributed to establish direct limits on the radio emission brightness temperature of ultracool objects such as TVLM 513–46546 (Forbrich and Berger 2009; 2013). Actually, this object has been the target of an astrometric campaign using the EVN to find the strongest constraints on possible companion masses and orbital periods (Gawroński et al. 2017; see Fig. 5.3). Other systems studied at high-resolution are the multiple substellar system VHS 1256-1257, where EVN observations helped to determine the spectral index of the radio emission (Guirado et al. 2018).

Clearly, more objects will be detected as the sensitivity of the arrays improve. The EVN (C-band) appears as an excellent tool to find compact radio emission in these unique systems which will be

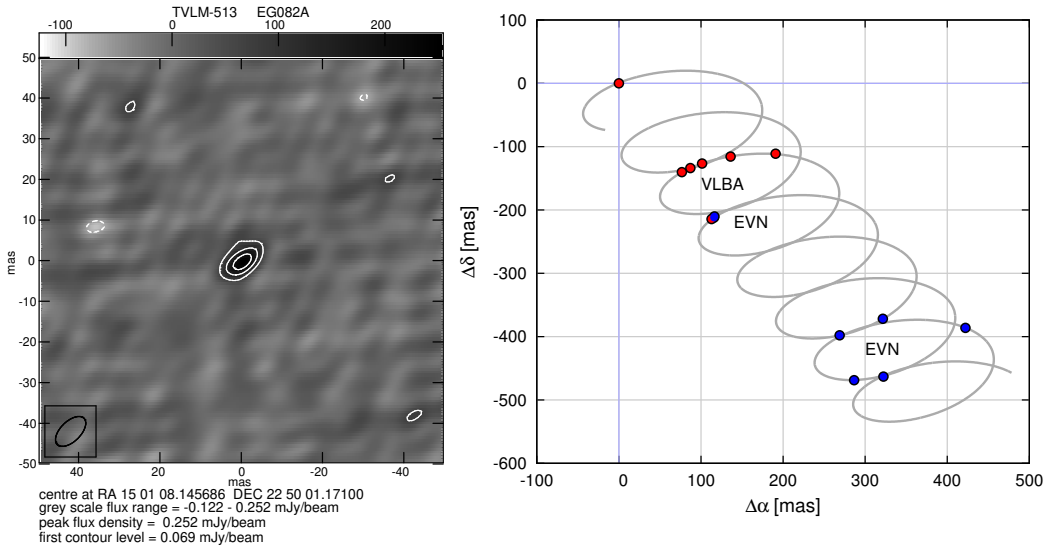

Figure 5.3: (left) 5 GHz EVN map of TVLM 513-46546. The first contour corresponds to the 3σ detection limit. (right) Sky-projected (proper motion + parallax) trajectory of TVLM 513–46546 (grey curve) overplotted with VLBA (red filled rectangles) and EVN detections (blue filled circles; adapted Fig. 1 and 5 from Gawroński et al. 2017).

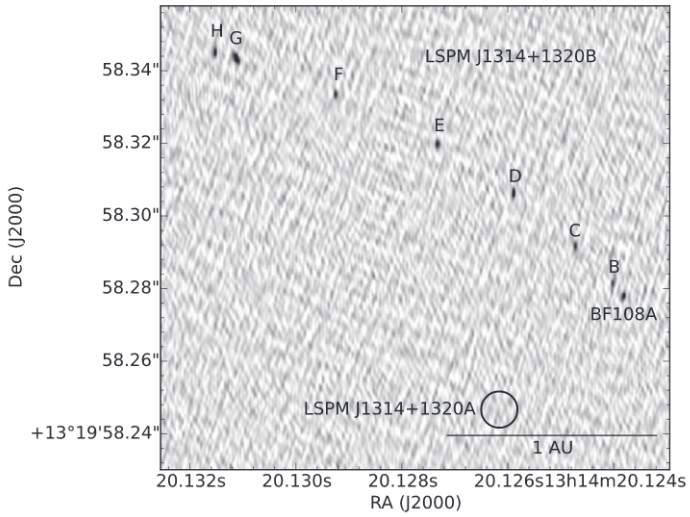

Figure 5.4: Co-added images of VLBA epochs of the ultracool binary LSPM J1314+1320A . The primary remains undetected at the circle of 5-mas radius. All eight detections of the secondary are clearly visible, and the shape of the orbit is recognizable (Forbrich et al. 2016). ©AAS. Reproduced with permission.

essential to observationally constrain the brightness temperature and, therefore, the nature of the radio emission. Of particular interest are double or multiple systems. In addition to enable astrometric studies aimed at determining the dynamical masses, high-resolution observations will determine whether the radio emission originates either in one or in both components. If both objects are radio emitters, they will probably have a similar rotation history (velocity and/or axis orientation), which has evolved to produce a magnetic field with similar intensity. On the contrary, if the radio emission comes essentially from one of the components, it will indicate the presence of underlying differences in the stellar rotation and/or different magnetic field configurations. An interesting avenue is the possibility stressed by Pineda et al. (2017), who suggested that the different radio emission properties in physically similar dwarf binary components (having same mass, luminosity, and temperature) might be due to the existence of a rocky planet around (only) one of them, which may induce a different magnetic configuration; therefore, the presence of the planet is the triggering factor of the radio emission. This is the case in at least two ultracool dwarf binaries: 2MASSI J0746425+200032 (Konopacky et al. 2010), and LSPM J1314+1320AB (Forbrich et al. 2016; see Fig. 5.4), which present radio emission in only one of the components, being primary targets in searches of Earth-mass planets.

Exoplanets

Radio wavelengths may provide direct detection of extrasolar giant planets (EGPs). While the ratio of the luminosities between an EGP and its parent star is very low in the optical, the radio luminosity ratio is not necessarily low. In principle, and mostly based on our knowledge of the Sun and Jupiter, this contrast is most favourable at decametre wavelengths, with the emission dominated by the cyclotron maser emission. This route to direct detection of exoplanets looks the most suitable, specially given the new, dedicated instruments at very low frequencies such as LOFAR or ASKAP. Complementary, EGP radio emission at GHz frequencies appears as a promising approach, as proved by the increasing number of radio detections of ultracool dwarf objects (Hallinan et al. 2008; McLean et al. 2011) with spectral types as cool as L3.5 (Router & Wolszczan 2012).

The angular resolution of VLBI systems can reach a few milliarseconds depending on the observing frequency. It provides an opportunity for direct observations of extrasolar planets in nearby planetary systems, which are similar to our Solar System. Using the direct detection/image of an extrasolar gas giant it could be possible to estimate its magnetic field strength and/or dynamical mass. This knowledge is crucial in our understanding of evolution and creation of Jupiter-like gas giants in planetary systems similar to ours. However, the main problem of detecting sub-stellar companions is the expected frequency of radio emission, if the emission processes are similar to what we observe in the Solar System. Radio observations of gas and ice giants in the Solar System show that dominant radio emission extends from kHz to 40 MHz. If the emission range is typical for all massive planets, only low frequency systems like LOFAR or SKA could likely detect radio emission from exoplanets. The frequency range of radio emission strongly depends on the exoplanet magnetic field strength and MHz waves are the result of G magnetic fields found in gas/ice giants in our Solar System.

Among a few possible processes that can generate radio emission in the planetary systems, three of them seem to be the most promising in terms of direct observations. The first mechanism assumes an interaction between the stellar wind and the planetary magnetosphere. The power of the radio emission in this process depends on the kinetic energy flux and spatial density of particles, that are impacting on the planet magnetopause (e.g Farrell, Desch & Zarka 1999). The second emission

process is an effect of the interaction between the magnetic energy flux of the interplanetary magnetic field with the planetary magnetosphere (e.g. Farrell et al. 2004). The third scenario assumes the existence of a moon around a planet. The volcanic activity of the moon fills the magnetosphere with matter that is ionised and accelerated by electric currents. The currents are inducted because of the difference between the gas giant rotation velocity and the moon orbital velocity (e.g Nichols 2012). In the Solar System it is impossible to distinguish which emission process dominates (the first or the second).

The theoretical models of the MHz radio emission from massive exoplanets were already investigated by several authors (see for a review Griessmeier, Zarka & Girrard 2011). It was shown, that it should be possible to detect low frequency radio emission from a few known massive exoplanets (e.g. ε Eri b or τ Boo b). However, despite many observational projects there is no confirmed detection of radio emission from exoplanets (e.g. George & Stevens 2007, Lecavelier des Etangs et al. 2013). Recent results presented by Kao et. al (2018) may shed some light on this mystery, as it seems the rapid rotation of sub-stellar objects is important in producing strong kG magnetic dipole systems. These authors present detections of radio emission from selected brown dwarfs which are strong and direct constraints on dynamo theory in gas giants located at the substellar-planetary boundary.

Recently it was also postulated that massive and young gas giants (<1 Gyr) could produce kG magnetic fields, which are able to produce radio emission at cm radio bands. It offers the possibility of the direct detection/discovery of exoplanets by existing VLBI systems (Katarzyński et al. 2016). The authors concentrated on the sample of young massive stars from the Solar neighborhood and showed that under reasonable assumptions it is possible to detect radio emission from putative massive gas giants located in those systems (Fig. 5.5). Actually, a recent result from Bastian et al. (2018) show a possible detection of radio emission from the planetary system ε Eri at cm-wavelengths. The results presented by Kao et. al (2018), Bastian et al. (2018), and Katarzyński et al. (2016) strongly indicate that VLBI systems could have a great importance and impact on current and future exoplanets studies.

5.1.3 Evolved stars

Mass loss / stellar winds

Radio observations have been a powerful tool to study, among other things, the atmosphere, winds and mass-loss of evolved stars, including Red Supergiants (RSGs), asymptotic giant branch stars and their evolution into planetary nebulae (PNe) as well as massive OB and WR stars. The evolution of AGB, RSG and more massive evolved stars is dictated by their mass-loss through strong stellar winds and is responsible for determining their final end-point. If ionised, these stellar winds produce detectable thermal radio emission. Mass-loss rates measured using a number of indicators (e.g. Hα/UV/radio) appear to disagree by significant amounts (e.g. Fullerton, Massa & Prinja, 2006) casting doubt on the expected evolution of the star. It is now believed that small-scale structure in the form of clumping is the reason for these discrepancies (e.g. Puls et al. 2006). Radio observations however, provide a distinct advantage in determining accurate mass-loss rates as they offer by-far the least model-dependent method and these can be interpreted directly from the radio flux density. Though massive stars are relatively faint, upgrades to existing interferometers such as increasing the bandwidth have improved the situation significantly. Radio surveys of Galactic clusters are now beginning to perform a census of radio emission from massive stellar winds through both focused surveys such as the *e*-MERLIN study of Cygnus OB2 (COBRaS: Morford et al. submitted; Fig. 5.6) and the ALMA investigation of Westerlund 1 (Fenech et al. 2018) as well as larger area and all-sky

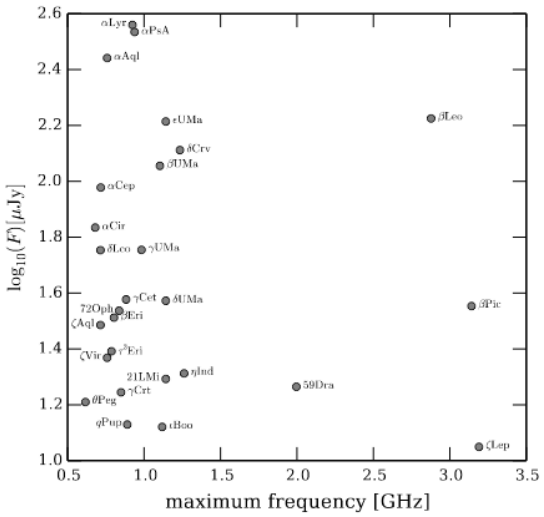

Figure 5.5: Expected radio emission from hypothetical object with masses M = 15 $M_{\rm Jup}$ located at the distance d = 1 AU around selected main-sequence A-type stars (Fig. 5, Katarzyński et al. 2016).

surveys such as the ASKAP SCORPIO (Umana et al. 2015) and EMU projects (Norris et al. 2011). Though observations of thermal stellar winds are brightness sensitivity limited, increased bandwidths along-side the correct combination of baselines (e.g. *e*-MERLIN with the inner EVN antennas) can be used to do more targeted observations of brighter objects to study potential variability and structure in the stellar winds.

Star spots

Evolution of starspots on various time scales allows us to investigate stellar differential rotation, activity cycles, and global magnetic fields, as well as to constitute the basis for our understanding of the stellar dynamo mechanism.

Starspots have been best-studied on Betelgeuse, starting ∼20 years ago with optical and IR interferometry. The radius of Betelgeuse has been resolved out to ∼ 125 mas (25 AU, or over 5× the optical radius) at λ6 cm using the VLA and *e*-MERLIN. The latter shows several surface brightness fluctuations of order 10% against the average temperature ∼ 2300 K at 5 cm. At wavelengths around ∼ 1 mm, ALMA has resolved one or two spots on Betelgeuse, Mira and a few other objects. In all these cases, the instrumental resolution is pushed to the limit and the spot sizes, and hence brightness temperature fluctuations, are not well defined; there could be smaller, brighter spots or even localised clusters of larger numbers of spots. It is intriguing to postulate a link with the low-filling-factor chromosphere measured for Betelgeuse (Harper et al. 2006) as well as with convection cell models (Chiavassa et al. 2010), but this has not been possible thus far. Adequate sensitivity at higher resolution can tackle these problems: 1) Tighter constraints on the numbers and nature of star spots. The optimal combination of resolution and sensitivity (considering atmospheric transmission as well as source properties) is around C-band, where Betelgeuse has a flux density of ∼ 2 mJy at 6 GHz. The *e*-MERLIN resolution places an upper limit of 50 mas on the spot sizes. If 10% fluctuations were smooth, this corresponds to 18 μ Jy per 15-mas resolution element, or 6μ Jy rms for a 3σ detection. This would be practical by combining *e*-MERLIN with EVN baselines out to ∼ 1000 km

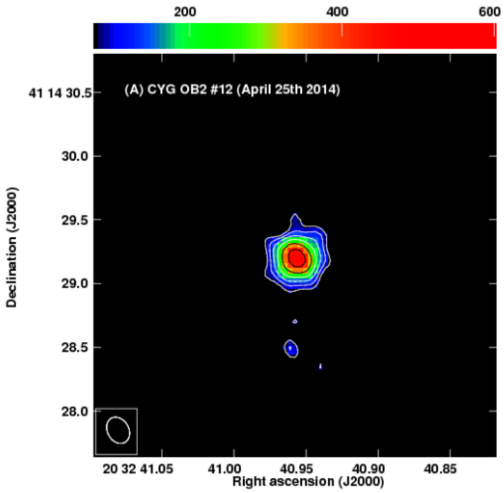

Figure 5.6: Image of one of the target sample stars from the COBRaS 21 cm *e*-MERLIN Legacy observations, Cyg OB2 #12, showing the first ever resolved image of its thermal emission at 21 cm (rms = 24 μJy/beam; Fig. 1 in Morford et al. 2016).

–of course, longer baselines would be valuable to investigate the existence of more compact, more extreme hotspots. 2) The hot-spots and stellar flux are variable and may have distinctive spectral indices. This is complicated by the wavelength dependence of the imaged surface, but this does offer the possibility to track disturbances by observing later epochs at longer wavelengths. Hence, for a single image, a fractional bandwidth of not more than 10% is best, from observations taken over a few days or weeks at most. On the other hand, if it was possible to observe at several frequencies using suitable combinations of EVN, *e*-MERLIN and the VLA, at suitable time intervals, this could trace disturbances propagating from 2–6 $R_\star$, on timescales from a week to many months, depending on whether radiative/recombination, shocks or bulk transport are involved (Harper & Linsky 1999).

There is evidence for a very low filling factor chromosphere in Betelgeuse (Harper et al. 2006) and the current estimates of radio hot spot brightness temperatures are based on > 50 mas resolution images. A very hot spot ($\sim$50 000 K, size of 2–3 mas) was measured on the AGB star W Hya by Vlemmings et al. (2017) using the long baselines of ALMA. It is possible that these mas-size features may be collections of much smaller, possibly even hotter spots with high enough non-thermal brightness to allow detection at cm-wavelengths with *e*-MERLIN combined with the shortest EVN baselines.

Colliding winds

Understanding binary interaction is also key for understanding stellar evolution and mass-loss and this is especially important considering the significant fraction of stars expected to undergo some binary interaction during their lifetime (50–70%). Interaction of stellar winds of massive binaries (OB type or WR) can produce shocks, defining a wind collision region (WCR) where particles are accelerated up to relativistic velocities. Within the WCR thermal radio emission is typically produced, but also non-thermal radio emission (from synchrotron radiation) which constitutes a suitable scenario for EVN/VLBI observations to spatially resolve such emission. Hence, precise distance and orbit, critical for modelling the WCR, have been determined for archetypical objects as

WR 140, a WR+O binary system which shows a bow-shaped arc emission that rotates as the highly eccentric orbit progresses (Dougherty et al. 2011). Recent results on the hierarchical triple system HD 167971 (an O-spectroscopic binary with a third O-star in a wider orbit; Sanchez et al. in press) demonstrate the ability of high-resolution VLBI maps to determine the orbit of the components relative to the bow-shock position, allowing to find an absolute astrometric solution for the complete system. The quadruple system in Cyg OB2 #5 is also a good example where the radio observations have been key to understanding the system as not all of the stars have been optically/spectrally identified and yet the non-thermal emission from the WCR clearly indicates their presence (e.g. Dzuib et al. 2013). In some cases, such as in the massive binary HD 93129A, VLBI observations were key to unveil the binary nature of the system due to the discovery of a powerful WCR (Benaglia et al. 2015).

Other systems include a variety of evolutionary stages e.g. O+O binaries, WR systems and probably shorter-lived stages such as Be systems. This will of course also include neutron-star and black-hole binary systems as well. As shown in some studies (De Becker et al. 2017), it is considered that WCR should not be a rare phenomenon in massive binary stars. Actually, these authors estimate that colliding-wind binaries may constitute a significant contributor of the Galactic cosmic rays; this finding increases the interest to widen the present census of massive binaries. Obviously, sensitive interferometers would be ideal, as VLBI should reveal the kinematics of the systems. Sampling at different baseline lengths, from tens to thousands kilometres to avoid resolving the emission, would be essential, as well as flexibility in frequency and time for multi-frequency and multi-epoch observations to observe at various orbital phases.

5.2 Stellar masers

The importance of spectral line observations concerning maser emission will be presented in this section. Owing to the increasing spectral resolution and sensitivity of VLBI arrays, many important results have been obtained in the last decades based on the VLBI observations of masers, naturally occurring sources of stimulated spectral line emission in the ISM. In the Milky Way, masers are typically found in star-forming regions and evolved stars. Being compact, bright, non-thermal emission structures they are ideal VLBI targets to be used for understanding physical parameters such as density and temperature, but also for accurate position measurements making them ideal astrometry targets. Maser astrometry is used for measuring the spiral structure of the Milky Way and the Galactic rotation curve. In the following subsections Galactic VLBI maser science of star-forming regions, evolved stars and astrometry are discussed. A summary of the astrophysical masers can be found in Gray (2012).

5.2.1 Masers in Star Forming Regions

High-mass stars have a large influence on the energetics of the gas and dust in the Galaxy via their bright UV emission and their strong winds which increase in their evolved stages, and finally by supernova explosions, through which they also dominate a galaxies' metal abundance. Understanding high-mass star formation is thus important for galaxy evolution on the large scales, and for a detailed view of stellar formation, including planetary system formation, on the small scales. In high-mass ($\geq 8 M_{\odot}$) star formation the accretion of matter onto the star has to overcome the strong radiation pressure released when the star commences hydrogen fusion. Among the various existing theories that explain the continuation of accretion or agglomeration of mass, high-resolution observations of

masers in rotating disk-like structures are favouring disks and accretion bursts implying an up-scaled version of low-mass star formation.

Molecular maser emission at cm wavelengths has been most useful to trace the early stages of the evolution of the protostar-disk-jet systems at milliarcsecond scales using VLBI. Sensitive VLBI observations show, mainly in association with intermediate- and high-mass protostars, thousands of maser spots forming microstructures that reveal the 3D kinematics of outflows and disks at small scale. This kind of observations have given a number of interesting results: the identification of new protoplanetary disks in YSOs at scales of tens of AU (Torrelles et al. 1998; see Fig. 5.7); the discovery of short-lived, episodic non-collimated outflow events (e.g., Torrelles et al. 2001, 2003; Surcis et al. 2014); detection of infall motions in accretion disks around massive protostars (Sanna et al. 2017); the imaging of young ($<$ 100 yr) small scale (a few 100 AU) bipolar jets of masers (Sanna et al. 2012, Torrelles et al. 2014); and even allowed us to analyze the small-scale (1-20 AU) structure of the micro bow-shocks (Uscanga et al. 2005; Trinidad et al. 2013).

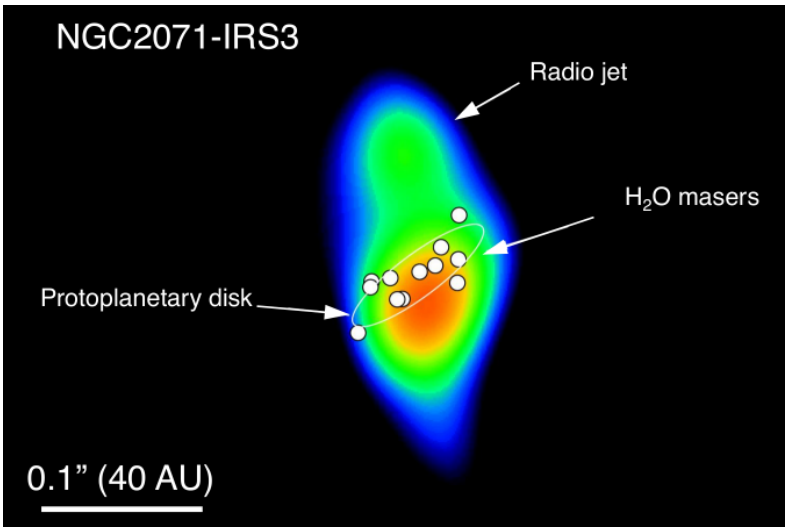

Figure 5.7: H_2O masers (white circles) tracing a protoplanetary disk of radius 20 AU, oriented perpendicular to the thermal radio jet associated with the protostar NGC 2071-IRS3 (Torrelles et al. 1998). ©AAS. Reproduced with permission.

With the rise of polarimetric measurements of star-forming cores, filaments, and, on small angular scales, disk-like structures and outflows, the importance of the magnetic field in star formation has been firmly established, though *how* and *how much* the magnetic field influences the star formation is still elusive to us. These open questions can be largely ascribed to the large difficulty of observing high-mass star-forming regions (HMSFRs). High-mass stars are rare, thus their birth-sites are generally found at large distances and therefore at small angular scales. In addition, they are enshrouded in large amount of natal dust and gas thus causing a high level of extinction and optical depth problems. Maser observations at the radio wavelengths ranges are not hindered by dust. The masers' compactness and high brightness temperatures allow one to use VLBI to accurately trace motions very close to the protostar, providing an unique way to search for rotating structures, such as disks, or outflows. VLBI polarimetry enables via morphology mapping and Zeeman splitting

measurements to determine 3D magnetic fields to investigate the connection between matter and magnetic field at $10-100$ AU scales.

Recently, the interest in the variability of maser emission associated with HMSFRs has skyrocketed by the discovery that many class II methanol masers vary periodically (Goedhart et al. 2014). Multi-transition maser observations (Fig. 5.8) yield precious information on the physical conditions where these masers operate, provided that good pumping models exist. The variability of astrophysical masers introduces a time-domain aspect which provides additional, and possibly unique, information of the star formation environment. Maser super bursts have now been observed in a few HMSFRs, such as the 6.7 GHz methanol maser emission flare in S255 NIRS3 (Moscadelli et al. 2017, Szymczak et al. 2018b), and appear to be connected to accretion bursts which could provide a solution to the radiative pressure limiting the accretion of matter onto the young stellar object (YSO) allowing it to grow in mass beyond $\sim$10 $M_\odot$. Water masers in jet-driven bow shocks provide additional information to episodic accretion (Burns et al. 2016). Only one case has been found so far where the 6.7 GHz methanol maser alternates with the 22 GHz water maser, that is the intermediate-mass young stellar object G107.298+5.639 (Szymczak et al. 2016). However, the origin of the anticorrelated variability of both lines is still under debate.

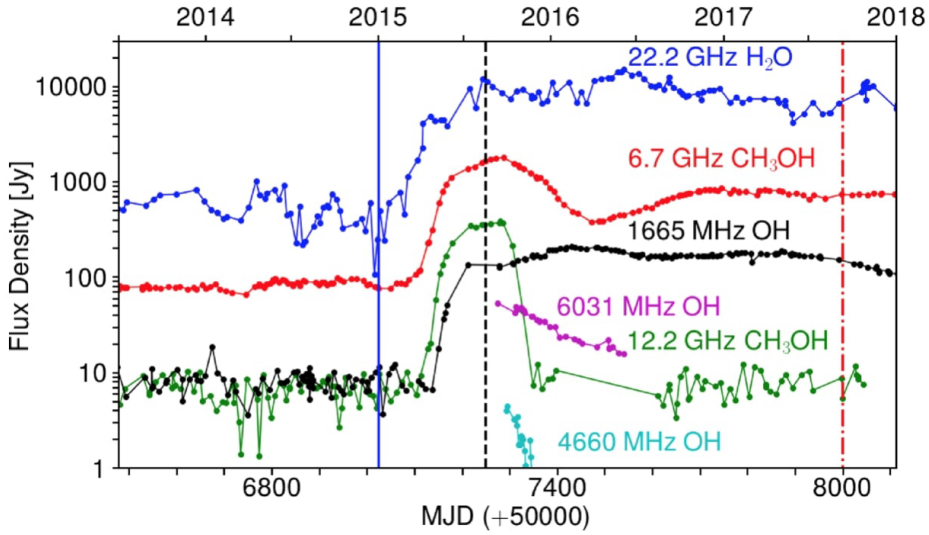

Figure 5.8: Time series of selected velocity channels of various maser species towards NGC 6334I measured with the 26 m telescope of the Hartebeesthoek Radio Astronomy Observatory (HartRAO) (Fig. 9, MacLeod et al. 2018). The blue vertical solid line indicates the onset of the outburst and the black dashed line marks the initial peak.

EVN research of masers in high-mass star-forming regions

High angular resolution observations of intense molecular masers, in particular SiO, H_2O, and CH_3OH, are crucial to resolve the gas kinematics at $10-100$ AU (requiring angular resolutions $< 0\farcs1$ at the typical distances >1 kpc of HMSFRs) around high-mass YSOs, where the accretion and ejection processes operate in close proximity. Combining maser VLBI data with (subarcsecond) interferometric observations of thermal (continuum and line) emission provides a very detailed

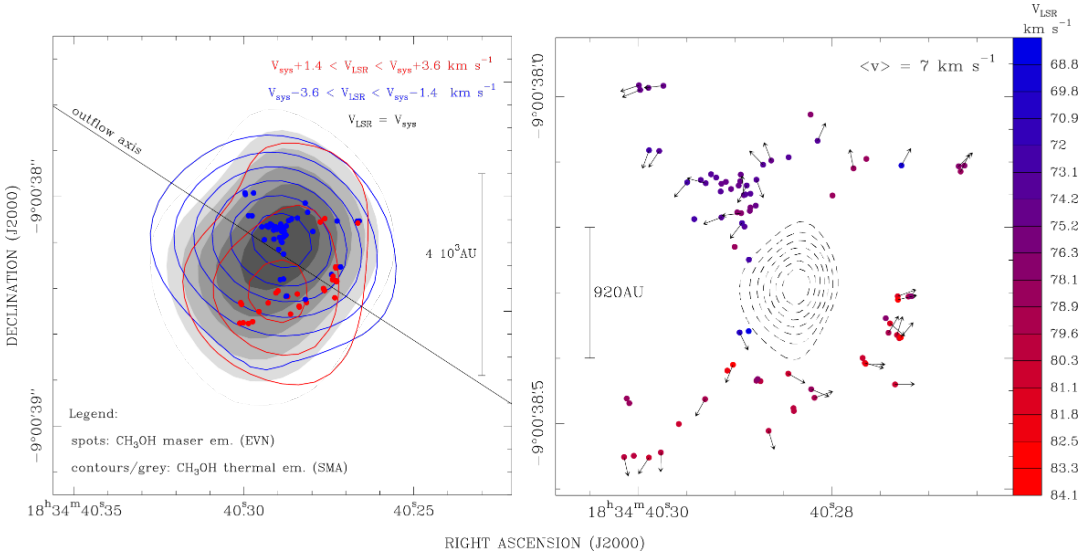

Figure 5.9: (left) Map of the CH_3OH (15_4-16_3) E line emission observed with the SMA towards G23.01-0.41. Adapted from Sanna et al. (2014), reproduced with permission ©ESO. (right) Positions and proper motions of the 6.7 GHz methanol masers (EVN) and VLA 1.3 cm continuum (dashed contours). Adapted from Sanna et al. (2010), reproduced with permission ©ESO.

view of the gas kinematics and physical conditions near the forming star. In general, it is found that water masers trace mass ejection in outflows or jets, while the methanol masers are more often located closer to the YSO, possibly in the disk-plane (perpendicular to the outflow axis) with kinematic patterns suggesting rotation. Recent EVN kinematics studies revealed that methanol masers might actually be related to an interface of the jet and disk regions rather than the disk-plane itself (Bartkiewicz et al. 2018). Unfortunately, detailed VLBI studies, which combine also other interferometric observations, have been performed only towards a small number of objects, so far, but have yielded very important observational clues. For example, submillimetre array observations reveal that the high-mass YSO G23.01−0.41, expected to be a ZAMS O9.5 star of ≈20 $M_\odot$, has a collimated bipolar molecular outflow at 0.1 pc scales, and, at the centre of the outflow, on a few 10^3 AU, the gas and dust distribution is flattened and oriented perpendicular to the outflow axis (Fig. 5.9). This is fully consistent with multi-epoch VLBA 22 GHz water and EVN 6.7 GHz methanol maser observations. On the one hand, the elongated distribution and collimated proper motions of the water masers suggest that they are tracing the YSO's jet driving the motion of the large scale molecular outflow. On the other hand, the 6.7 GHz methanol masers are distributed at radii from a few 100 AU to a few 10^3 AU around the YSO, and trace the envelope-disk kinematics (Fig. 5.9). Their proper motions are quite complex and can be explained in terms of a composition of slow (ca. 4 km s^{-1} in amplitude) motions of radial expansion and rotation about an axis approximately parallel to the water maser jet.

The EVN has given a particularly strong contribution to the magnetic field studies in HMSFRs. Observations of the polarised emission of different maser species have provided magnetic field measures in different ambient conditions within HMSFRs, at a spatial resolution unachievable with any other kind of observations. Perhaps, the most groundbreaking and unique results have been the EVN observations of polarised emission of 6.7 GHz methanol masers. Surcis et al. (2013, 2015,

2019) and Dall'Olio et al. (2017) showed that these masers, located close to the accretion disks and in the ambient medium between disks and outflows, have preferred magnetic field orientations along the outflow axis. By combining the magnetic field morphology with the gas motions, measured simultaneously from the same data set, Sanna et al. (2015b) have proved, for the first time, that gas with low turbulence moves along the magnetic field lines (Fig. 5.10). In the last 10 years Zeeman splitting measurements of 6.7 GHz methanol masers (in particularly with the EVN) have become more common. However, only since 2018 these measurements can be further used to estimate the magnetic field strength (measured to be of the order of 1-10 mG), thanks to the newly calculated Landé g-factors for all the hyperfine transitions of the methanol molecule (Lankhaar et al. 2018). This provides important input for theoretical models of star formation.

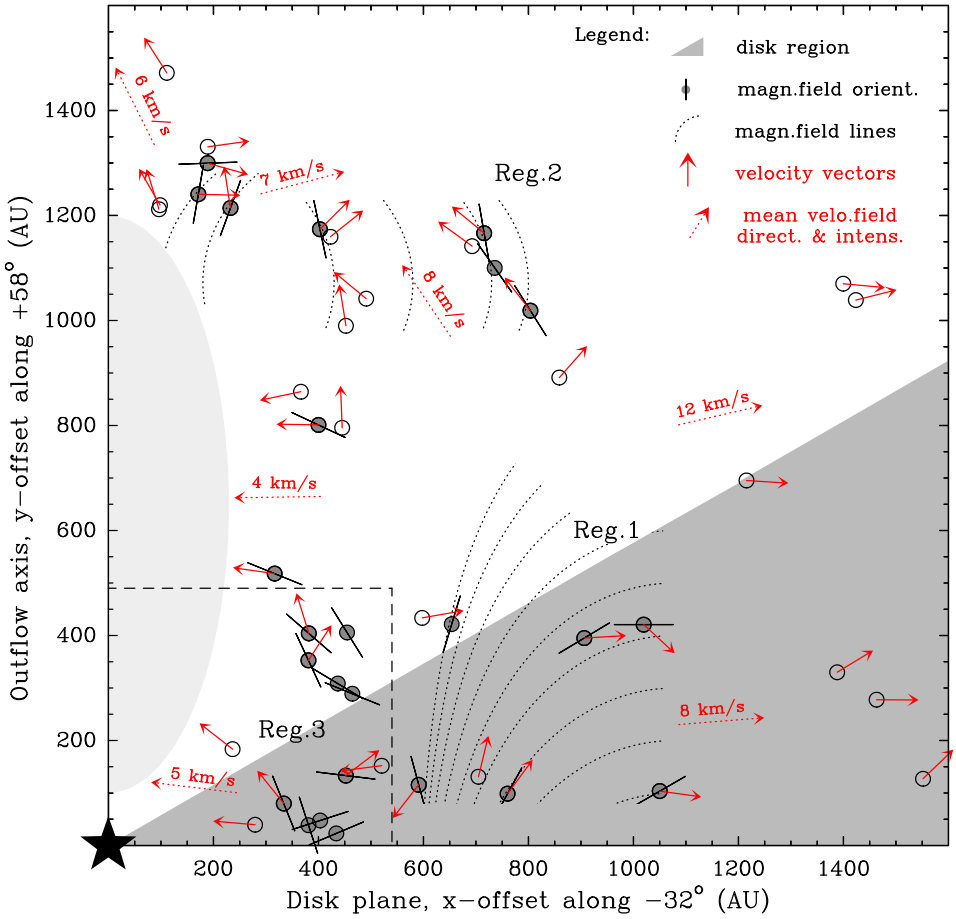

Figure 5.10: Gas dynamics and magnetic field configuration revealed within the inner 2000 AU of a high-mass YSO in G023.01−00.41 (Sanna et al. 2015b). Empty and solid dots in the vicinity of the hot molecular core centre (star) mark the 6.7 GHz CH_3OH masers emitting unpolarised and polarised light, respectively. Arrows correspond to the local direction of the velocity of the masers and bars represent magnetic field vectors. Magnetic field lines (dotted lines) are extrapolated from the average behaviour of the magnetic field vectors. Adapted from Sanna et al. (2015b), reproduced with permission ©ESO.

Small scale magnetic fields can be also studied with water maser VLBI polarimetry. Goddi et al. (2017) revealed a complex picture of water maser polarisation using full polarimetric VLBA observations: on scales of thousands AU, the magnetic field traced by polarised water maser is aligned with the synchrotron jet in W3(H_2O), though, on 10s to 100s of AU, a misalignment between the magnetic field and the velocity vectors was revealed, and ascribed to the compression of the field component along the shock front. Similar studies are also done using the EVN, of particular interest is the case of W75N(B): a 6-year EVN monitoring project has been investigating the correlation between outflow collimation and magnetic field, both measured using water maser emission, around a number of massive young stellar objects in the region (e.g. Surcis et al. 2014).

The EVN is the proper instrument to take up the challenge of understanding the cause of maser variability. The focus of high resolution maser studies should be directed first to those star forming regions where the maser variability is predictable and repeatable, e.g. the periodic class II methanol masers. The first of such observations, a single epoch VLBA observation, was done towards G9.62+0.20E, where not only class II methanol masers show periodic flaring but also the 1665 and 1667 MHz OH masers (Sanna et al. 2015a; Goedhart et al. 2018). Although this source is not observable with the EVN, there are a few periodic methanol maser sources that have similar methanol maser flare profiles which can be studied with the EVN (Szymczak et al. 2016, 2018a; Olech et al. 2018).

In all 6.7 GHz observations the software XF-kind correlator (SFXC) at JIVE allowed easily to achieve a sufficient spectral resolution of 0.9 $\mathrm{km\,s^{-1}}$ (e.g. the 2 MHz bandwidth divided onto 1024 spectral channels). However, future studies with a higher spectral resolution may bring surprises like discovering amplification-bounded masers (Bartkiewicz et al. 2016). Recently, Takefuji et al. (2016) measured temporal coherent lengths of water maser emission in bright HMSFRs using the 34-m dish, indicating that coherent maser emission might exist. This could be confirmed by high spatial resolution (to isolate individual masers) and ultra-high spectral resolution to reveal the underlying (not Gaussian/broadened) line shape. Measuring coherent maser emission would reveal fundamental properties of the maser phenomenon itself.

5.2.2 Masers around Evolved Stars

Most circumstellar masers are associated with the Asymptotic Giant Branch (AGB) evolutionary phase, when low and intermediate mass stars climb the AGB, or with more massive stars in the Red Supergiant stage. In the process of transforming into PNe or supernovae (SN) such stars evolve within a few years and lose their final outer layers very rapidly. In the molecular material that is flowing away from variable, O-rich stars, OH, H_2O and SiO masers occur. The various maser transitions sample different parts of the circumstellar envelope (CSE) tracing different physical processes (Gray et al. 2016). Aside from understanding this evolutionary stellar phase per se, studying the expulsion of matter from evolved stars is important since it is responsible for the bulk of dust and many CHNOPS-containing molecules in the ISM. Currently, it is suspected that stellar pulsations, large convective cells and magnetic fields are important, but no conclusive observational tests have yet been performed on a wide enough sample. Once enough dust forms, radiation pressure drives the wind away from the star – which continues accelerating for 100s $R_\star$ (the optical photospheric radius), beyond the ability of current models to explain. High-resolution imaging shows that much of the wind is concentrated in dense clumps. Distinguishing their properties (density, temperature etc.) from the surroundings is vital to deduce the chemistry, composition and total mass loss, and the prospects for survival of dust and molecules into the ISM. Also in this topic, masers are an ideal tool

for these studies as the bright, compact emission allows positions and line widths to be measured with an order of magnitude more precision than thermal lines.

EVN research of masers in evolved stars

SiO masers (43, 86 and 129 GHz) arise at 2–5 $R_\star$, where the stellar atmosphere becomes optically thin in the IR and internal pulsations give rise to shocks, and are thus used to study the impact of stellar pulsations. Proper motions of SiO masers reveal complex motions including outflow and infall. Large samples of SiO proper motions are required to disentangle various velocity fields from the net radial expansion, ballistic ejection and correlate these with polarisation measures and dust formation. Furthermore, the comparison of the absolute positions of the emission distribution of different SiO maser lines, may reveal whether such masers are radiatively or collisionally pumped and constrain the IR radiation field (Fig. 5.11, left panel).

Water masers at 22 GHz (collisionally pumped) trace rapid changing conditions in evolved star CSEs from about 5–50 $R_\star$. They occur in clouds of typical radius $R_\star$, which, if traced back to the star assuming radial expansion, implies a birth radius of 0.05–0.1 $R_\star$. If individual (sub-mas) maser components can be resolved without losing more extended flux, the nature of maser beaming can be investigated and clouds can be distinguished as either quiescent or a shocked slab. The latter are rarer and variability often affects the entire maser shell, on a timescale too fast for shocks to propagate, implying radiative heating effects. Changes between tangential and radial beaming are due to fluctuations in the velocity field, in turn a product of the efficiency of conversion of radiative energy into acceleration, also demonstrated by velocity drifts of maser features. More detailed water maser beaming and proper motion studies are needed to investigate these mechanisms.

OH 1612-MHz masers form shells, undergoing uniform expansion, at hundreds $R_\star$. In many cases their intensity has a straightforward relationship with the stellar period allowing the phase-lag method to be used for distance determination (Etoka et al. 2018). The precise determination of distances with this method relies on an accurate estimate of the size and geometry of the OH 1612 MHz shell, which is often aspherical. Appropriate resolution and high-sensitivity imaging are required in order to constrain these two parameters. While intermediate/short baselines are important to image, in particular, the faint external emission, proved to be extended towards OH/IR stars, the zooming power of the EVN is crucial to image and study the intrinsically compact regions associated with e.g. flaring events. Surprisingly, the OH mainline (1665/7 MHz) masers often overlap the outer 22 GHz H_2O maser shell (e.g. Etoka et al. 2017), although the former require much cooler, less dense conditions, probably emanating from inter-clump gas. The magnetic fields in the CSE are found to be important, as can be seen from the highly ordered linear polarisation vectors observed in the OH maser components of *o* Ceti (Fig. 5.11, right panel).

The expanding frequency coverage of VLBI, alongside ALMA, provides observations of multiple maser transitions in CSEs. Computational advances have led to recent maser models which can infer physical conditions such as temperature and number density, based on which lines co-propagate or are segregated. Maser polarisation and Zeeman splitting show that there is a stellar-centred magnetic field. This could be poloidal, Solar-type or toroidal (field strength $\propto r^\alpha$, where α is 3, 2 or 1 respectively), and could be well-constrained by measuring the field strength using maser species sampling a wide range of distances from the star. Thus far, only a few measurements are available, mostly from different objects or without accurate distances, favouring a lower value of α (Vlemmings et al. 2005, Leal-Ferreira et al. 2013).

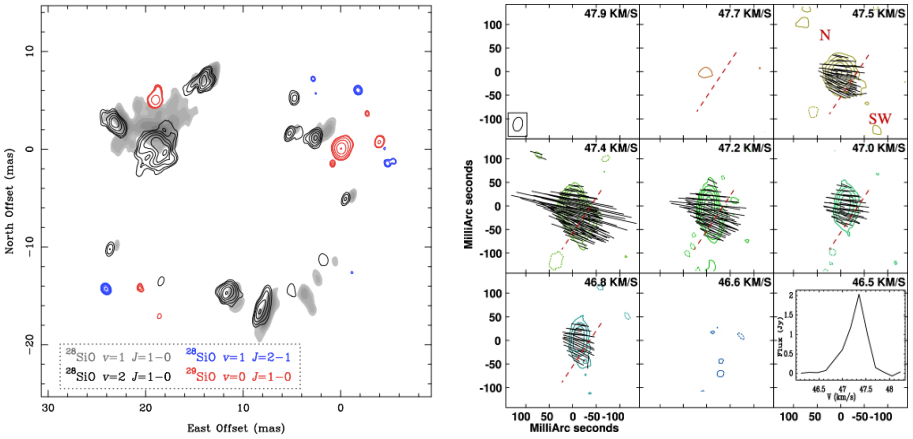

Figure 5.11: (left) Comparison of several maser lines of SiO in the AGB star IRC +10011. Adapted from Soria-Ruiz et al. (2004), reproduced with permission ©ESO. (right) EVN-*e*-MERLIN Stokes I contour maps of the 1665 MHz flaring emission towards o Ceti with the relative polarimetric information overlaid (Fig. 11, Etoka et al. 2017).

5.2.3 Maser Astrometry

The Milky Way offers unique possibilities to study structure formation in the Universe. Despite the location of our Solar System in the Galactic plane, we can infer how the Galaxy evolved and possibly was subject to minor and major mergers. In principle, this can be done by measuring the dynamics of stellar populations and characterising their age and metallicity. Astrometric campaigns in the radio, using VLBI, can address these topics, and are complementary to the impressive output data coming from ESA's optical astrometry satellite *Gaia*. Besides the structure of the Galaxy, direct distance measurements are also of fundamental importance to derive fundamental properties of astrophysical objects. Mass, luminosity, accretion and mass-loss rates, inferred pressures and energy balances all depend critically on accurate distances.

In the plane of the Galaxy, precise distances and proper motion measurements are very difficult to obtain, and *Gaia* distances are limited to a few kpc due to interstellar extinction. Thus, optical astrometry will not have the capability to measure the spiral structure (or infer the Hubble type) of the Milky Way, and neither will it resolve the kinematics of the inner Galaxy, including the Galactic bar and bulge. These structures are of particular interest to understand the nature and history of the Milky Way. VLBI astrometry is therefore fundamental for measuring the large-scale parameters of the Galaxy, such as the distance to the Galactic centre and rotation curve (Reid & Honma 2014). For the latter, measuring stellar motions and distances in the outer Galaxy is also important.

The distance and proper motions of HMSFRs, which are deeply embedded in dense molecular clouds, can be measured through water, methanol and SiO maser astrometry. Such campaigns map out the spiral structure of the Galaxy (Fig. 5.13, left panel) and can also provide a census of the current high-mass star formation across the Galaxy. The tremendous reach of VLBI astrometry includes masers in the far side of the Galaxy, with distances up to 20 kpc (Sanna et al. 2017). Water and in particular 6.7 GHz methanol masers are closely associated with those sites where high-mass stars are born (e.g. Menten et al. 1991, Breen et al. 2013), and these sites are located along the Galactic spiral arms, maser observations also yield the dynamic scale (size and rotation) of the Galaxy. It should be noted that low mass star formation does not produce bright enough (stable)

masers for astrometry, though VLBI astrometry can be performed by observing the non-thermal emission from pre-main sequence stars (see more in Section 5.1.1).

Many AGB stars also contain maser emission and could be used for VLBI astrometry (see Fig. 5.12). Unlike HMSFRs that are still confined to the natal molecular clouds, evolved stars move through the Galaxy on dynamically relaxed, collision free orbits that may still carry information on their birth events, possibly Giga years ago. The least obscured AGB stars, the Mira variables and carbon stars, are observable by *Gaia* too, but *Gaia*'s astrometry cannot be expected to provide much information about the enigmatic dynamics of the inner Galaxy.

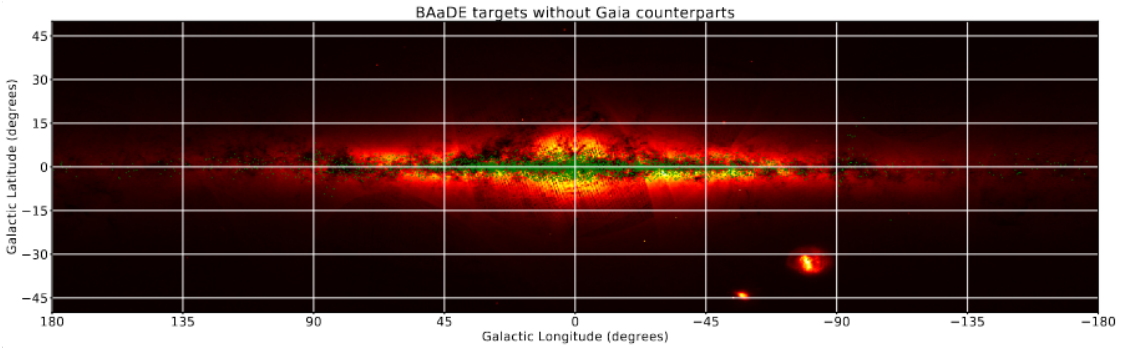

Figure 5.12: Plot of *Gaia* detections towards the inner Galaxy. The green symbols are BAaDE, SiO maser star targets for which no *Gaia* counterpart can be identified. Adapted from Quiroga-Nuñez et al. (2018), reproduced with permission ©ESO.

EVN research of maser astrometry

The scientific impact of maser astrometry has been very substantial; papers that summarise the Galactic structure are widely recognised across many astronomical fields (Reid & Honma 2014). In addition, results that give robust distances for otherwise obscured targets, often have very high citations. For example, many recent ALMA papers quote distances for evolved stars and star-forming regions based on VLBI. For such embedded objects, it can be expected that *Gaia* will only improve the distances for a very limited number of them, and recent comparisons suggest that *Gaia* and VLBI results are consistent (*Gaia* Collaboration, 2016) and complementary .

The highest impact programme on maser astrometry so far have been the BeSSel and VERA projects (Brunthaler et al. 2011, Reid et al. 2014, 2019, Kobayashi et al. 2003). They started by targeting the brightest methanol (12 GHz) and water masers (22 GHz) with the VLBA (BeSSel) and water (22 GHz) and SiO (43 GHz) masers with the Japanese VLBI array (VERA). It was complemented by some 6.7 GHz masers observed with the EVN (Rygl et al. 2010, 2012). With the new C-band receivers on the VLBA the BeSSel sample has been doubled by including observations of ubiquitous 6.7 GHz masers. We must note, some of this work could in principle have been done equally well with the EVN, which is maybe harder to calibrate for astrometry but possibly more sensitive. But, it requires a large commitment in observing time outside the normal EVN sessions.

The astrometry of evolved stars started with results on OH masers (Vlemmings & van Langevelde 2007). But, at 1.6 GHz (18 cm) the distance range accessible is restricted, because of the limited (intrinsic) brightness of the masers. However, higher accuracy measurements will become possible when multiple close calibrators can be observed simultaneously with high signal-to-noise ratio (Rioja et al. 2017). The most relevant results are however still obtained through water masers, most of these

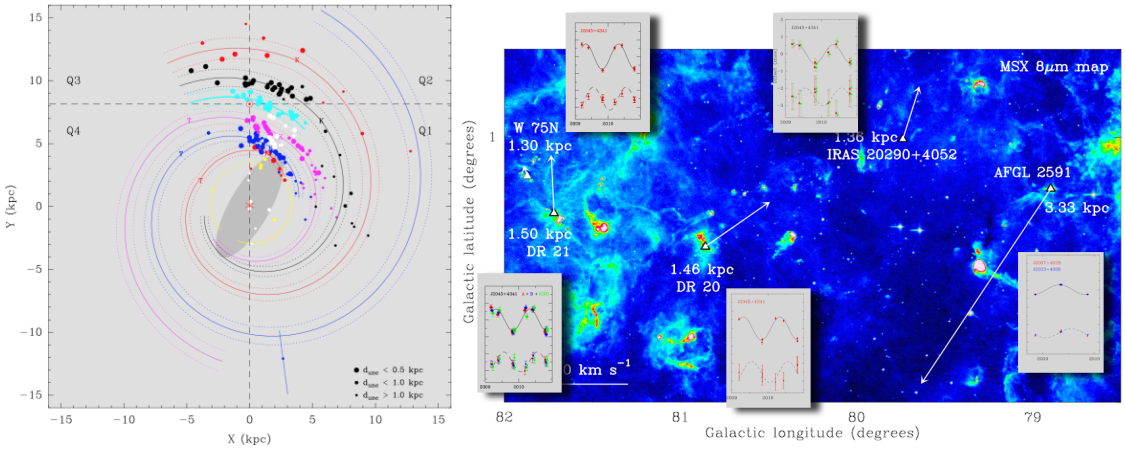

Figure 5.13: (left) The location of high-mass star forming regions in the Galaxy outlines a spiral arm pattern (Reid et al. 2019). ©AAS. Reproduced with permission. (right) Distances to star-forming regions in Cygnus X complex: the insets show the fitted parallax sinoids in R.A. and declination of the star-forming regions, while the white arrows (on the *MSX* map) indicate the 3D space motions of the star-forming regions (indicated by white triangles). Adapted from Rygl et al. (2012), reproduced with permission ©ESO.

observed with VERA and the VLBA. SiO masers may be more relevant in the future. Recently, the VLA and ALMA were used to establish a very large sample ($> 10,000$) of SiO masers (the BAaDE project, Sjouwerman et al. 2017). In principle, VLBI could uniquely measure the stellar motions in the inner Galaxy through these sources, although the requirements for calibration and monitoring are very severe; switching times would be under a minute and source variability is expected to occur on time scales of a month. Absolute positions of SiO and water masers in AGB stars and proto PNe can be used to study various structures, such as bipolar jets or the stellar envelope (see e.g. Desmurs et al 2007), to understand the evolutionary scenario of these stars. Also, a lack of water in the equatorial regions of the inner CSE may be explained by the presence of a companion star.

The EVN made a considerable impact by providing astrometry of methanol masers at 6.7 GHz (Rygl et al. 2010, 2012, see Fig. 5.13, right panel), when it was still the only VLBI array with many receivers covering the 5 cm transition. Various other projects measured the kinematics of methanol masers, by monitoring experiments not optimised for parallax as described in Section 5.2.1. Here the EVN excels by making many weak features visible and tracing them over a few years.

5.2.4 Technical requirements and synergies

The three most-pressing limitations of the EVN for stellar studies nowadays are:

(i) The array's sensitivities, especially for continuum and polarisation studies. Quiescent, disc-averaged stellar radio emission is very weak. Most of the projects described above require continuum sensitivities better than a few μJy/beam, and they are natural targets for connected interferometers as the JVLA or *e*-MERLIN. Present EVN sensitivity may reach 5-10 μJy (1 σ) for reasonable integration times at cm-wavelengths and assuming the object is not overresolved. This leaves little room for the EVN in terms of sensitivity to thermal stellar emission, restricted to the brightest objects. Nevertheless, VLBI appears as the only technique able to provide the submilliarcsecond

resolution necessary to map the fine details of coronal or collinding-wind structures combined with the submilliarcsecond precise astrometry needed for measuring the distance to star forming regions or the reflex motion induced by substellar objects. Sensitive observations with good spectral resolution are necessary for maser observations especially for polarisation studies. To detect at 5σ typical low circular polarisation fraction (>0.3%) for maser emission with flux >1 Jy beam^{-1} it is necessary to reach an rms level of 0.6 mJy beam^{-1} per channel that currently requires 167 hr and 417 hr of observing time at C- and K-band, respectively (see Surcis et al. 2014, 2019).

(ii) The poor *uv*-coverage in the north–south direction; this is the same orientation as the Galactic plane where many HMSFRs and AGB stars are. Extending the EVN baselines to AVN telescopes will be a giant step in terms of building the *uv*-coverage, providing access to a complete census of star forming regions and stellar moving groups, and opening the inner Galaxy up for unparalleled VLBI exploration.

(iii) The lack of short baselines. EVN technical improvements should be addressed to provide μJy/beam sensitivity in short-spaced baselines not to overresolve the stellar objects. Compatibility with *e*-MERLIN is a sensible recommendation which would add baselines of $<$100 km, allowing significant contributions in every single stellar project; e.g. the EVN plus shorter spacings will be invaluable in resolving non-thermal flares or possibly chromospheric hot spots with sufficient detail to monitor their origins and role in binary evolution and mass loss.

Further technical considerations

The EVN's limitations for some projects like astrometry stem mostly from the sparse telescope availability outside of the EVN sessions that is required to sample the parallax sinusoid properly to distinguish the parallax imprint from the proper motion, the high slewing times that make phase-reference observations very slow, and the currently scarce high frequency coverage. For these reasons most astrometric results today are coming from the US VLBA or the Japanese VERA, which have antennas able to perform rapid phase referencing and operate all year. The EVN, providing an unparalleled sensitivity at the lower frequencies thanks to 70–105 m dishes, is frequently used for astrometric projects that do not require special scheduling constraints. Improvement on the astrometric precision (down to a few μas) may come more from the use of techniques as the Multiview phase-referencing (Rioja et al. 2017), which achieves a more effective treatment of (atmospheric) systematic errors, relaxing the constraints of the angular separation of the reference source(s). On the longer term, EVN antennas equipped with phase array feeds will allow multiview-like observations for virtually any target-calibrator separation.

The BRAND broad band receiver should cover the range from 1 to 15 GHz to permit simultaneous observations of methanol (6.7 and 12 GHz) in full polarisation mode allowing for the derivation of physical conditions such as temperatures and densities in dense regions of high-mass star-formation sites. However, one must remember, the line sensitivity will be worse. Ideally, the receiver coverage could include also the 22 GHz water masers and 1.6665/7 GHz OH masers as these masers are often coexistent in HMSFRs and AGB stars and provide information on various structures with different kinematic properties. Simultaneous imaging of multi-maser transitions for a number epochs during a flare will permit to accurately track the flare evolution at various spatial positions without any alignment complications (in time and space) and derive physical conditions. Also, for AGB stars, where water and OH are spatially in close proximity, here proper motions might reveal how velocity gradients, number densities and temperature contrasts constrain pumping. The broad band receiver will improve significantly continuum measurements, which perhaps might not be enough for detecting the stellar continuum in AGB stars, but it would enable the obtention of rigorous spectral

information both for coherent flaring and incoherent gyrosynchrotron or synchrotron radiation. Additionally, the astrometric precision of the EVN would be improved via more precise atmospheric calibrations and the possibility of using weaker position reference sources with a smaller separation to the target. It should be underlined that still much is to be gained by increasing the spectral resolution (contrary to the wide band observations mentioned above), in particular for maser polarimetry, which requires spectral resolution of 100 kHz to resolve the methanol hyperfine structure and improve Zeeman splitting measurements, and for detecting coherent maser emission, for which the spectral resolution has to be as fine as 1 kHz. Observations of coherent maser emission require a spectral resolution range of $<$1 Hz to many kHz to resolve the homogeneous width at all levels of saturation.

Most SiO maser VLBI studies have been carried out with the VLBA, the KVN and the VERA (e.g. Gonidakis et al. 2010, Oyama et al. 2016, Yun et al. 2016). But, the future installation of new K/Q/W receivers on several EVN antennas, especially the large dishes, will boost the SiO science. Simultaneous maser observations of water and several lines of SiO, will help understanding the mass loss mechanism at work in AGB shells. Playing a role in possible future SiO maser astrometry may require additional receiver efforts for those EVN telescopes that are able to reach millimetre wavelengths with capability of fast-switching. This proposed stellar astrometry is a different application from simultaneously observing H_2O and SiO masers, it would aim to use more sensitive K band calibrator observations to measure the relative position of SiO masers at Q band. Such a technique for transferring phase corrections between bands was developed by Rioja & Dodson (2011). SiO astrometry is interesting for the CSE per se, but will be an almost unique method to measure accurate distances and proper motion of AGB stars in the Galactic bar and bulge (see section Astrometry). Also higher Class I methanol masers transitions (e.g. 25 GHz, 36 GHz) are of great scientific relevance for HMSFR studies, though they might be resolved on the longest (intercontinental) EVN baselines.

For a complete picture of the circumstellar envelopes, covering a wide range in size scales from tens of mas down to hundreds of mas, VLBI has to be combined with shorter baselines, and complemented with single dish and connected interferometers. *e*-MERLIN can provide the short baselines at 22 GHz, but for the higher SiO frequencies intermediate baselines, between 36 km (VLA) and a few hundred kilometres are a world-wide problem. Connected mm interferometers (ALMA/NOEMA) can observe several SiO and water maser lines together with the stellar continuum, and provide a unique method to spatially correlate the maser emission with the stellar photosphere. In general, there is the importance of combining interferometric continuum and molecular emission with maser VLBI measurements to obtain a complete picture for the (usually) dense regions where optical observations are impossible. In addition, much is expected from the future synergy with the SKA, if it will have VLBI capabilities, improving the sensitivity and *uv*-coverage towards the inner Galaxy. In particular, the SKA-MID which would include the 6.7 GHz methanol (band 5a) and the 12 GHz methanol transition (band 5b, possibly extending to the 22 GHz water maser line) could allow for new methanol astrometry of southern targets (see Loinard et al. 2015).

Classical synergies between single dish and VLBI keep being vital for the variability of masers, with different classes of variability like periodically variable and bursts. Therefore, the rapid VLBI response organised through trigger proposals is important.

Finally, intensive and complex data processing schemes to derive parallaxes from VLBI monitor campaigns as well as the bulk of the all EVN data reduction, rely mostly on classic AIPS and ParselTongue. It is hoped that such processing schemes are more easily implemented and executed in the future with the growing VLBI functionality of CASA for which VLBI reduction pipelines are already existing (Janssen et al. 2019).

5.2.5 Summary

The use of the VLBI technique is already extended throughout the complete H−R diagram, enabling studies of the radio emission of all sorts of stellar objects from protoplanetary disks to evolved stars, including main-sequence stars, brown dwarfs, and exoplanets. Maser science has provided fundamental insights in the workings of high-mass star formation by measuring the magnetic fields and gas dynamics down to size scales of 100 AU, the mass expulsion in evolved stars from a few $R_\star$ out to hundreds $R_\star$ together with magnetic field measurements, and has mapped out the spiral structure of our Galaxy and improved our knowledge of fundamental parameters such as the distance to the Galactic centre and the Galactic rotation curve. The EVN has played a role in many stellar projects, however, still it can be used more. These studies are rather time-consuming, often requiring more than one epoch with rather long on-source time, resulting in a limited number of stellar targets that are studied by VLBI. Often, in astrometry studies there is a need to observe outside the standard EVN sessions. Future EVN, and VLBI in general, observations with improved sensitivity through the inclusion of more (and larger) dishes, improved *uv*-coverage (in particular in the north-south axis via AVN and SKA), increased frequency coverage, increased receiver bandwidth allowing for simultaneous observations of several maser transitions will allow VLBI science to extend to fainter targets, improved astrometry, and a better Galactic plane coverage which is crucial for understanding Galactic dynamics. Thus, there is still much to be explored in the Milky Way using the EVN.

REFERENCES

ALMA Partnership, Brogan, C. L., Pérez, L. M. et al., 2015, *ApJ*, **808**, L3
Anglada, G., Rodríguez, L. F., & Carrasco-González, C. 2015, PoS(AASKA14), 121
Anglada , G., Rodríguez, L. F., & Carrasco-González, C. 2018, *A&A Rev*, **26**, 3
Araudo, A. T., et al. 2007, *A&A*, **476**, 1289
Azulay, R. et al., 2015, *A&A*, **578**, A16
Azulay, R. et al., 2017, *A&A*, **607**, A10
Bally, J., 2008, *Handbook of Star Forming Regions*, **Volume I, 4**, 459
Baraffe, I. et al., 1998, *A&A*, **337**, 403
Bartkiewicz, A. et al., 2018, *Proceedings IAU Symposium: Astrophysical Masers: Unlocking the Mysteries of the Universe*, **336**, 211
Bartel, N. et al., 2015, *Class. Quant. Grav.*, **32**, 224021
Bastian, T.S., Benz, A.O., & Gary, D.E., 1998, *ARAA*, **36**, 131
Bastian, T. S. et al., 2018, *ApJ*, **857**, 2, 133
Benaglia, P. et al., 2015, *A&A*, **579**, A99
Breen, S.L. et al., 2013, *MNRAS*, **435**, 524
Brunthaler, A. et al., 2011, *AN*, **332**, 461
Burns, R.A. et al., 2016, *MNRAS*, **460**, 283
Bartkiewicz, A., Szymczak, M., & van Langevelde, 2016, *A&A*, **587**, A104
Carrasco-González, C., et al. 2010, *Science*, **330**, 1209
Chabrier, G. et al., 2000, *ApJ*, **542**, 464
Chiavassa, A. et al., 2010, *A&A*, **515**, A12
Cotton, W.D., Perrin, G., & Lopez, B., 2008, *A&A*, **477**, 853
Dall'Olio, D. et al., 2017, *A&A*, **607**, A111
De Becker, M. et al., 2017, *A&A*, **600**, A47

Desmurs, J.F. et al., 2007, *A&A*, **468**, 189
Dobashi, K. et al., 2005, *PASJ*, **57**, S1
Dougherty, S. M., Trenton, V., & Beasley, A. J., 2011, *BSRSL*, **80**, 658
Dzib, S. A. et al., 2018, *ApJ*, **853**, 99
Dzib, S. A. et al., 2016, *ApJ*, **826**, 201
Etoka, S. et al., 2017, *MNRAS*, **468**, 1703
Etoka, S. et al., 2018, *Proceedings IAU Symposium: Astrophysical Masers: Unlocking the Mysteries of the Universe*, **336**, 381
Farrell, W. M., Desch, M. D., & Zarka, P., 1999, *J. Geophys. Res.*, **104**, 14025
Farrell, W. M. et al., 2004, *Planet. Space Sci.*, **52**, 1469
Feigelson, E. D., & Montmerle, T. 1985, *ApJ*, **289**, L19
Fenech, D. M. et al., 2018, *A&A*, **617**, A137
Forbrich, J. et al., 2016, *ApJ*, **827**, 22
Fomalont, E., & Kopeikin, S. M., 2003, *AJ*, **598**, 704
Forbrich, J., & Berger, E., 2009, *ApJ*, **706**, L205
Forbrich, J., Berger, E., & Reid, M.J., 2013, *ApJ*, **777**, 70
Fullerton, A. W., Massa D. L., & Prinja, R. K., 2006, *ApJ*, **637**, 1025
Gaia Collaboration, Brown, A.G.A., Vallenari, A. et al., 2016, *A&A*, **595**, A2
Galli, P. A. B. et al., 2018, *ApJ*, **859**, 33
Garay, G., et al. 2003, *ApJ*, **587**, 739
Gawroński, M.P., Goździewski, K. & Katarzyński, K., 2017, *MNRAS*, **466**, 4211
George, S. J., & Stevens, I. R., 2007, *MNRAS*, **382**, 455
Ghez, A. M., Neugebauer, G, & Matthews, K., 1993, *AJ*, **106**, 2005
Goddi, C. et al., 2017, *A&A*, **597**, A43
Goedhart, S. et al., 2014, *MNRAS*, **437**, 1808
Goedhart, S. et al., 2018, *Proceedings IAU Symposium: Astrophysical Masers: Unlocking the Mysteries of the Universe*, **336**, 225
Gonidakis, I., Diamond, P.J., & Kemball, A.J., 2010, *MNRAS*, **406**, 395
Greaves, J. S. et al., 2008, *MNRAS*, **391**, L74
Gray, M.D., 2012, *Maser Sources in Astrophysics*, Cambridge, UK: Cambridge University Press
Gray, M.D. et al., 2016, *MNRAS*, **456**, 374
Griessmeier J.-M., Zarka P., & Girard J. N., 2011, *Radio Sci.*, **46**, RS0F09
Güdel, M., Guinan, E. F., & Skinner, S. L., 1998, *ASP Conf. Ser.*, **154**, 1041
Güdel, M. et al., 1989, *A&A*, **220**, L5
Guirado, J. C. et al., 1997, *ApJ*, **490**, 835
Guirado, J. C. et al., 2018, *A&A*, **610**, A23
Gwinn, C. R. et al., 1997, *ApJ*, **485**, 87
Hallinan, G. et al., 2008, *ApJ*, **684**, 64
Harper, G. & Brown, A., 2006, *ApJ*, **646**, 1179
Hoare, M. G. 2006, *ApJ*, **649**, 856
Janssen, M. et al., 2019, *A&A*, **626**, A75
Kao, M. M. et al., 2016, *ApJ*, **818**, 24
Kao, M. M. et al., 2018, *ApJS*, **237**, 25
Katarzyński, K., Gawroński, M., & Gozdziewski, K., 2016, *MNRAS*, **461**, 929
Kenyon, S. J., Gómez, M., & Whitney, B. A., 2008, *Handbook of Star Forming Regions*, **Volume I, 4**, 405

Khodachenko, M. L. et al., 2007, *Astrobiology*, **7**, 167
Kobayashi, H. et al., 2003, *ASP Conference Series*, **306**, 367
Konopacky, Q. M. et al., 2010, *ApJ*, **711**, 1087
Kounkel, M. et al., 2017, *ApJ*, **834**, 142
Lammer, H. et al., 2007, *Astrobiology*, **7**, 185
Lankhaar, B. et al., 2018, *Nature Astronomy*, **2**, 145
Lecavelier des Etangs, A. et al., 2013, *A&A*, **552**, A65
Leal-Ferreira, M.L. et al., 2013, *A&A*, **554**, A134
Lestrade, J.-F. et al., 1995, *A&A*, **304**, 182
Loinard, L., 2013, *Advancing the Physics of Cosmic Distances*, **289**, 36
Loinard, L. et al., 2015, *PoS["AASKA14"]166*
Macías, E., et al. 2016, *ApJ*, **829**, 1
MacLeod, G. C. et al., 2018, *MNRAS*, **478**, 1077
Matthews, L. D., 2013, *PASP*, **125**, 313
McLean, M. et al., 2011, *ApJ*, **741**, 27
Melis, C. et al., 2014, *Science*, **345**, 1029
Menten, K. M. 1991, *ApJ*, **380**, L75
Moscadelli, L. et al., 2017, *A&A*, **600**, L8
Morford, J. C. et al., 2016, *MNRAS*, **463**, 763
Muench, A. et al., 2008, *Handbook of Star Forming Regions*, **Volume I, 4**, 483
Nichols J. D., 2012, *MNRAS*, **427**, L75
Norris, Ray P. et al., 2011, *PASA*, **28**, 215
O'Dell, C. R. et al., 2008, *Handbook of Star Forming Regions*, **Volume I, 4**, 544
Ortiz-León, G. N. et al., 2018, *ApJ*, **865**, 73
Ortiz-León, G. N. et al., 2017, *ApJ*, **834**, 143
Ortiz-León, G. N. et al., 2017, *ApJ*, **834**, 141
Osten, R. A., & Bastian, T. S., 2006, *ApJ*, **637**, 1016
Osten, R. A., & Bastian, T. S., 2008, *ApJ*, **674**, 1078
Oyama, T. et al., 2016, *PASJ*, **68**, 105
Palau, A., et al. 2014, *MNRAS*, **444**, 833
Parker, E. N., 1955, *ApJ*, **122**, 293
Pérez, L. M. et al., 2016, *Science*, **353**, 1519
Pineda, J. S., Hallinan, G., & Kao, M. M., 2017, *ApJ*, **846**, 75
Puls, J. et al., 2006, *A&A*, **454**, 625
Quiroga-Nuñez, L.H. et al., 2018, *Proceedings IAU Symposium: Astrophysical Masers: Unlocking the Mysteries of the Universe*, **336**, 184
Reid, M.J., & Honma, M., 2014, *ARA&A*, **52**, 339
Reid, M.J., & Menten, K.M., 1990. *ApJ*, **360**, L51
Reid, M.J. et al., 2014, *ApJ*, **783**, 130
Reid, M.J. et al., 2019, *ApJ*, **885**, 131
Reid, M.J. et al., 2007, *ApJ*, **664**, 950
Reiners, A. & Basri, G., 2007, *ApJ*, **656**, 1121
Richards, A.M.S. et al., 2012, *A&A*, **546**, A16
Rioja, M. et al., 2017, *AJ*, **153**, 105
Rioja, M.J., & Dodson, R., 2011, *AJ*, **141**, 114
Rodríguez-Kamenetzky, A., et al. 2017, *ApJ*, **851**, 16

Route, M., & Wolszczan, A., 2012, *ApJL*, **747**, L2
Ryde, N. et al., 2006, *ApJ*, **637**, 1040
Rygl, K.L.J. et al., 2010, *A&A*, **511**, A2
Rygl, K.L.J. et al., 2012, *A&A*, **539**, A79
Sanna, A. et al., 2010, *A&A*, **517**, A78
Sanna, A. et al., 2012, *ApJ*, **745**, 191
Sanna, A. et al., 2014, *A&A*, **565**, A34
Sanna, A. et al., 2015a, *ApJ*, **804**, L2
Sanna, A. et al., 2015b, *A&A*, **583**, L3
Sanna, A. et al., 2017, *Science*, **358**, 227
Segura, A. et al., 2010, *AsBio*, **10**, 751
Sjouwerman, L.O. et al., 2017, *Proceedings IAU Symposium: The Multi-Messenger Astrophysics of the Galactic Centre*, **322**, 103
Somers, G., & Pinsonneault, M. H., 2015, *ApJ*, **807**, 174
Soria-Ruiz, R. et al., 2004, *A&A*, **426**, 131
Straižys, V., Černis, K., & Bartašiūtė, S. 2003, *A&A*, **405**, 585
Straižys, V., Černis, K., & Bartašiūtė, S. 1996, *Baltic Astronomy*, **5**, 125
Surcis, G. et al., 2013, *A&A*, **556**, A73
Surcis, G. et al., 2014, *A&A*, **565**, L8
Surcis, G. et al., 2015, *A&A*, **578**, A102
Surcis, G. et al., 2019, *A&A*, **623**, A130
Szymczak, M. et al., 2016, *MNRAS*, **459**, L56
Szymczak, M. et al., 2018a, *MNRAS*, **474**, 219
Szymczak, M. et al., 2018b, *A&A*, **617**, A80
Takefuji, K., Imai, H., & Sekido, M., 2016, *PASJ*, **68**, 86
Tognelli E., Prada Moroni P. G., Degl'Innocenti S., 2011, *A&A*, **533**, A109
Torrelles, J.M. et al., 2014, *MNRAS*, **442**, 148
Torrelles, J.M. et al., 1998, *ApJ*, **505**, 756
Torrelles, J.M. et al., 2001, *Nature*, **411**, 277
Torrelles, J.M. et al., 2003, *ApJ*, **598**, L115
Torres, C. A. O. et al., 2008, *Handbook of Star Forming Regions*, **Vol. 5.**, 757
Trinidad, M.A. et al., 2013, *MNRAS*, **430**, 1309
Uscanga, L. et al., 2005, *ApJ*, **634**, 468
Umana, G. et al., 2015, *MNRAS*, **454**, 902
Villadsen, J. et al., 2017, *AAS Meeting 229*, id.116.05
Vlemmings, W.H.T., van Langevelde, H.J., & Diamond, P.J., 2005, *A&A*, **434**, 1029
Vlemmings, W.H.T., & van Langevelde, H. J., 2007, *A&A*, **472**, 547
Vlemmings, W. et al., 2017, *Nature Astronomy*, **1**, 848
Yun, Y. et al., 2016, *ApJ*, **822**, 3
Zhu, Z. et al., 2018a, *ASP Conf. Ser*, **517**, 193
Zhu, Z., Andrews, S. M., & Isella, A. 2018b, *MNRAS*, **479**, 1850
Zuckerman, B., & Song, I., 2004, *ARA&A*, **42**, 685